Generated Pattern Current in Electrochemical Water Treatment: Overcoming DC Limitations in Electrocoagulation, Electrooxidation, Electrochlorination, and Electrodialysis

Ibrahim Karakoc

GigaPulse Energy, Izmir, Turkey

ibrahim@gigapulse.energy

Abstract

Electrochemical water treatment processes—including electrocoagulation, electrooxidation, electrochlorination, and electrodialysis—are constrained by the temporal limitations of direct current excitation. DC operation induces electrode passivation, mass-transfer depletion at the electrode–electrolyte interface, suboptimal reactive oxygen species generation, and concentration polarization in membrane systems. Generated Pattern Current (GPC), a pre-engineered electrochemical control methodology implemented through the Dynamic Defined Pattern Charging (DDPC) framework, addresses these limitations through the deliberate temporal structuring of current delivery. Grounded in Jensen's inequality for nonlinear systems—$f(\bar{x}) \neq \bar{f}(x)$—GPC exploits the nonlinear response of electrochemical interfaces to produce superior process outcomes at identical average current densities. This paper presents a unified theoretical framework for GPC application across the four principal electrochemical water treatment domains. For electrocoagulation, GPC periodically disrupts the passivating oxide layer on sacrificial electrodes, extending operational lifetime and maintaining Faradaic efficiency. For electrooxidation, GPC modulates the hydroxyl radical generation cycle through synchronized high-current and low-current phases, enhancing oxidative yield per unit energy. For electrochlorination, GPC optimizes anodic chlorine evolution while suppressing deleterious chlorate formation. For electrodialysis, GPC mitigates concentration polarization and membrane scaling through precision-tuned pulsed excitation. A reference implementation via the GP R Module (GigaPulse Energy industrial retrofit unit) is described, offering researchers an open platform for experimental validation. This work expands the GPC theoretical canon to encompass water treatment, a domain of substantial global importance.

Keywords: Generated Pattern Current; Dynamic Defined Pattern Charging; Electrocoagulation; Electrooxidation; Electrochlorination; Electrodialysis; Electrode Passivation; Water Treatment; Jensen's Inequality

1. Introduction

Access to safe water is among the most pressing global challenges of the twenty-first century. Electrochemical water treatment technologies have emerged as compelling alternatives to conventional chemical methods, offering compact footprints, minimal reagent consumption, operational flexibility, and compatibility with distributed renewable energy sources [1, 2]. The four principal electrochemical modalities—electrocoagulation, electrooxidation and its advanced oxidation variants, electrochlorination, and electrodialysis—address complementary aspects of the treatment spectrum, from particulate and colloidal removal to dissolved organic degradation, pathogen inactivation, and desalination [3, 4].

Despite their distinct mechanisms, these processes share a common operational paradigm: all are driven by a direct current power supply delivering a nominally constant current or voltage to an electrochemical cell. This paradigm, while simple and well-characterized, imposes fundamental constraints that have not been resolved by advances in electrode materials, reactor geometry, or process integration alone. In electrocoagulation, sustained DC operation leads to the progressive formation of a passivating surface layer on the sacrificial anode, reducing Faradaic efficiency and increasing the voltage required to maintain target current density [1, 5]. In electrooxidation, DC excitation depletes the diffusion layer adjacent to the anode, limiting the replenishment of organic substrate and suppressing the effective •OH generation rate below its thermodynamic potential [9, 10]. In electrochlorination, the continuous application of a fixed anodic potential drives sequential oxidation of chlorine species toward undesired chlorate and perchlorate products [15, 16]. In electrodialysis, sustained ion flux under DC conditions creates concentration polarization at membrane interfaces, precipitating scale formation and accelerating membrane fouling [17, 18].

The temporal dimension of current delivery—the manner in which current is structured as a function of time—has been identified as a critical but underexplored control variable in each of these domains. Pulsed direct current (PDC), alternating pulsed current, and polarity reversal

techniques have demonstrated measurable improvements in electrocoagulation performance [5, 6, 7]. Pulse-potential electrooxidation has shown up to 50% improvement in energy efficiency for organic oxidation [11]. Pulsed electrodialysis (PED) has reduced membrane scaling and energy consumption by 30–36% compared with continuous operation [17, 20]. These findings collectively indicate that the temporal structure of current is not a neutral operational parameter but a determinant of process outcome.

Generated Pattern Current (GPC), established through the Dynamic Defined Pattern Charging (DDPC) framework, represents a systematic theoretical and engineering advance over ad hoc pulsing approaches. GPC patterns are pre-engineered, fixed-geometry temporal current structures stored in a look-up table (LUT) and selected prior to operation based on process chemistry. Unlike simple pulse or polarity reversal strategies, GPC encodes precise amplitude, frequency, phase, and duty cycle profiles into process-specific GPC forms tailored to the target electrochemical interface [25]. The theoretical foundation of GPC rests on Jensen's inequality for convex and nonlinear functions: for a nonlinear response function f and a time-varying input I(t), the time-averaged output $\bar{f}(I(t))$ differs from the output evaluated at the time-averaged input $f(\bar{I})$. This distinction—quantified as the Jensen gap—provides a rigorous basis for understanding how temporal current structure modulates process outcomes in systems with nonlinear electrode kinetics [24].

The GPC framework has been developed and applied across a growing range of electrochemical domains. Prior publications in this series have established GPC applications in battery formation and optimization [26, 27], hybrid capacitor conditioning [28—see SSRN 6431938], semiconductor processing [see SSRN 6437961], electroplating [28], water electrolysis for hydrogen production [29], anodizing, electrodissolution, graphene exfoliation, and electrochemical synthesis [30]. The present paper extends this framework to the domain of electrochemical water treatment, providing unified theoretical analysis and a reference implementation pathway for experimental validation.

This paper is organized as follows. Section 2 establishes the theoretical foundations of GPC and the Jensen gap as applied to electrochemical systems. Section 3 presents the GPC framework for electrocoagulation. Section 4 addresses GPC-enhanced electrooxidation and advanced oxidation. Section 5 covers GPC-modulated electrochlorination. Section 6 analyzes GPC in electrodialysis. Section 7 describes the GigaPulse Lab reference implementation. Section 8 presents validation frameworks. Section 9 concludes.

2. Theoretical Foundations: GPC and Jensen's Inequality in Water Treatment Systems

2.1 Jensen's Inequality and Nonlinear Electrochemical Response

The mathematical basis for GPC's advantage over DC operation is provided by Jensen's inequality. For a convex function f defined on a real interval, the inequality states:

$$f(E[X]) \leq E[f(X)]$$

where E[·] denotes expectation. For a concave function, the inequality is reversed. In the electrochemical context, X represents the instantaneous current I(t) and $E[X] = \bar{I}$ is its time average [24]. Electrochemical reaction rates—including anodic dissolution in electrocoagulation, •OH generation in electrooxidation, chlorine evolution in electrochlorination, and ion flux in electrodialysis—are governed by Butler–Volmer kinetics, which are inherently nonlinear in overpotential and, through Ohm's law, in current [22]. Consequently, a temporally structured current I(t) with the same time-average as a DC current $\bar{I}$ will, in general, produce different time-averaged reaction rates. The direction and magnitude of this deviation—the Jensen gap—depends on the local convexity of the electrochemical response function.

For processes exhibiting convex rate-overpotential relationships (e.g., •OH generation at high anodic overpotentials), GPC patterns that alternate between high-amplitude excitation phases and low-amplitude rest phases can exploit Jensen's inequality to elevate the time-averaged reaction rate above that achievable by DC at the same average current. For processes exhibiting concave relationships or those limited by surface-layer accumulation rather than kinetics, GPC patterns can be designed to periodically drive the system beyond the passivation threshold, clearing the electrode surface and restoring kinetic efficiency [5, 6].

2.2 GPC Pattern Architecture

A GPC pattern is a pre-engineered, fixed-geometry temporal current profile stored in a LUT within the GigaPulse Lab control system. The pattern is characterized by its shape function $s(t) \in [0, 1]$, amplitude A, offset I_0, duty cycle D, and frequency f_p, such that the instantaneous current is:

$$I(t) = I_0 + A \cdot s(t)$$

The time average $\langle I(t) \rangle = \bar{I}$ is preserved across all pattern configurations, ensuring that Faradaic charge balance is maintained at the process design point. The shape function s(t) is purpose-engineered for the target electrochemical process through systematic analysis of its reaction kinetics, mass-transfer time constants, and interfacial dynamics. No generic or pre-existing template is applied; each GPC form is produced through first-principles engineering specific to the process chemistry. Feedback parameters—amplitude A, offset I_0, and duty cycle D—are adjusted in real time by the GP R Module closed-loop controller based on impedance $Z(\omega)$, equivalent series resistance (ESR), and electrochemical stress index σ measurements; however, the geometric shape of s(t) is never modified during operation. This distinction—feedback-controlled scalar parameters operating on a fixed geometric form—is fundamental to GPC and distinguishes it from adaptive waveform synthesis approaches [25].

2.3 GigaPulse Lab System Topology

The GP R Module functions as the control and intelligence layer of the GPC system. It does not directly interface with the electrochemical cell. The system architecture is as follows: The GP R Module transmits reference current I_ref(t) and reference voltage V_ref(t) signals to the industrial rectifier (Power Source); the Power Source applies the corresponding current or voltage to the electrochemical cell; feedback signals—measured current I, voltage V, and temperature T—are returned from the Power Source to GP R Module; The GP R Module computes real-time process metrics (impedance, ESR, stress index σ, and dESR/dt) and updates I_ref and V_ref via closed-loop control logic; process completion is determined by the GP R Module based on threshold conditions. This topology ensures electrical isolation between the control system and the cell, enables retrofit deployment on any existing industrial rectifier infrastructure, and supports real-time pattern adaptation without hardware modification.

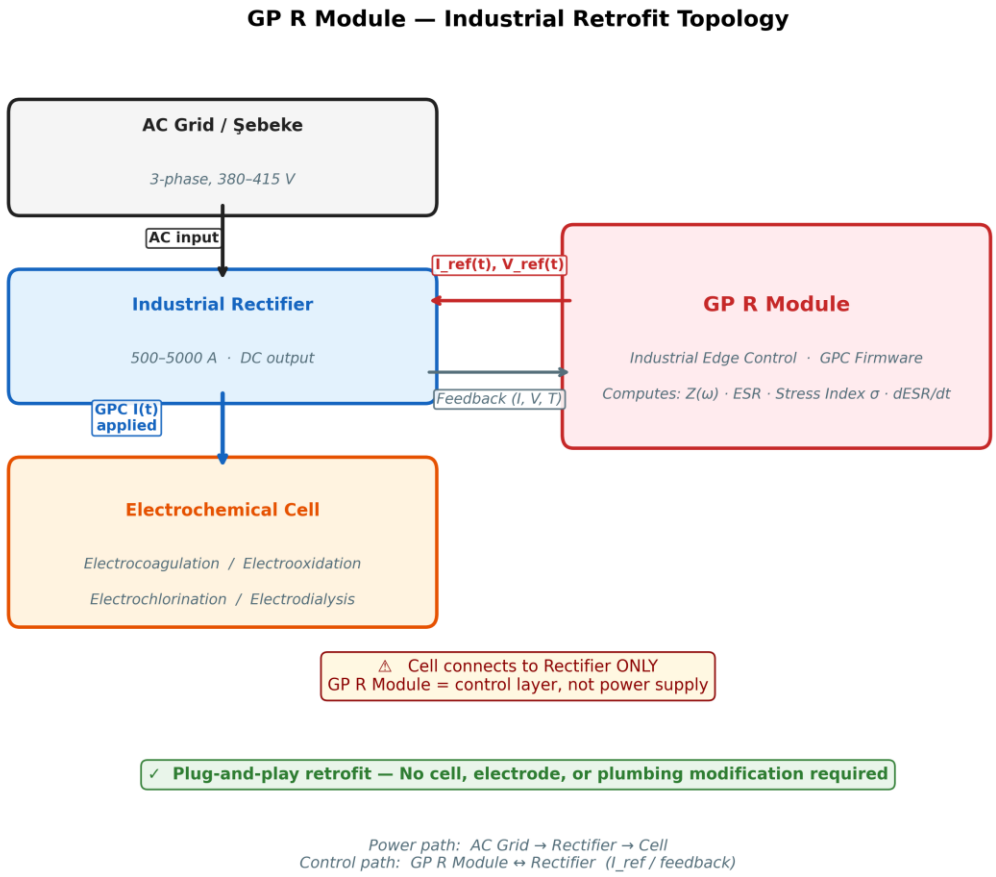

Figure 3. GP R Module industrial retrofit topology for electrochemical water treatment. Power path: AC Grid → Rectifier → Cell. Control path: GP R Module ↔ Rectifier (I_ref / feedback). The cell connects to the rectifier only. No cell, electrode, or plumbing modification is required.

Figure 1. Electrode behavior under DC versus GPC excitation in electrocoagulation. (a) Schematic of progressive passivation layer formation under DC, showing increasing surface resistance over time. (b) GPC pattern-driven periodic disruption of the passivating layer, enabling surface renewal and sustained Faradaic efficiency. (c) Comparative performance metrics: DC versus GPC at equivalent average current density.

3. GPC-Enhanced Electrocoagulation

3.1 Electrode Passivation in electrocoagulation: The DC Limitation

In electrocoagulation, the sacrificial anode—typically aluminum or iron—undergoes electrochemical dissolution, releasing metal cations (Al^{3+} or Fe^{2+}/Fe^{3+}) that hydrolyze to form

metal hydroxide coagulants in solution. These coagulants destabilize colloidal particles and suspended matter through charge neutralization, sweep flocculation, and adsorption, enabling removal by sedimentation or flotation [1, 2]. Under sustained DC operation, however, the progressive oxidation of the anode surface produces a dense, poorly conducting metal oxide/hydroxide layer that impedes further dissolution [5]. This passivating layer—typically comprising goethite, lepidocrocite, and magnetite in iron systems, and aluminum hydroxide polymorphs in aluminum systems—can reduce Faradaic efficiency from near-unity to below 50% within tens of minutes of operation, requiring a compensatory increase in cell voltage to maintain target current density and thereby increasing specific energy consumption [6, 7].

Polarity reversal and alternating pulsed current have been demonstrated to mitigate passivation by periodically exchanging the roles of anode and cathode, exposing a fresh electrode surface and promoting H_2 evolution at the previously anodic surface, which mechanically disrupts the passivating layer [5, 6]. However, these simple approaches are implemented without systematic optimization of the reversal geometry, frequency, or amplitude profile. Suboptimal reversal parameters can reduce coagulant generation per unit charge, decrease net contaminant removal, and increase sludge volume [5].

3.2 GPC Mechanism in Electrocoagulation

GPC addresses electrode passivation in electrocoagulation through two synergistic mechanisms. First, the process-specific GPC form applies high-amplitude excitation phases of engineered duration and magnitude, sufficient to electrochemically reduce the surface oxide layer or to promote localized hydrogen evolution at incipient passivation sites, followed by a structured low-amplitude or off-phase during which fresh electrolyte diffuses to the electrode surface. The timing parameters τ_on and τ_off are pre-engineered to match the characteristic time constants of oxide nucleation ($\tau\_nucleate$) and electrolyte replenishment (τ_diff) at the electrode surface:

$$\tau\_on \approx \tau\_passivate / 2 \; ; \; \tau\_off \geq \tau\_diff$$

This pre-engineered timing prevents the passivating layer from reaching the critical thickness δ_crit at which it begins to impede ionic transport. Second, GPC patterns that include a low-amplitude cathodic phase (negative offset) within the pattern cycle achieve in-situ electrochemical reduction of surface oxides without requiring complete polarity reversal, preserving net anodic dissolution while suppressing passivation.

The theoretical improvement in coagulant generation rate under GPC relative to DC can be expressed through the Faradaic efficiency ratio:

$$\eta_{F,GPC} / \eta_{F,DC} = [1 - \theta_{GPC}(t)] / [1 - \theta_{DC}(t)]$$

where $\theta(t)$ is the fractional surface coverage by the passivating layer, which under GPC is maintained at a lower time-averaged value through periodic renewal. The energy benefit arises from the reduction in required cell voltage at constant average current: $V_{cell,GPC} < V_{cell,DC}$ for the same $\langle I \rangle$ when $\theta_{GPC} < \theta_{DC}$ [7].

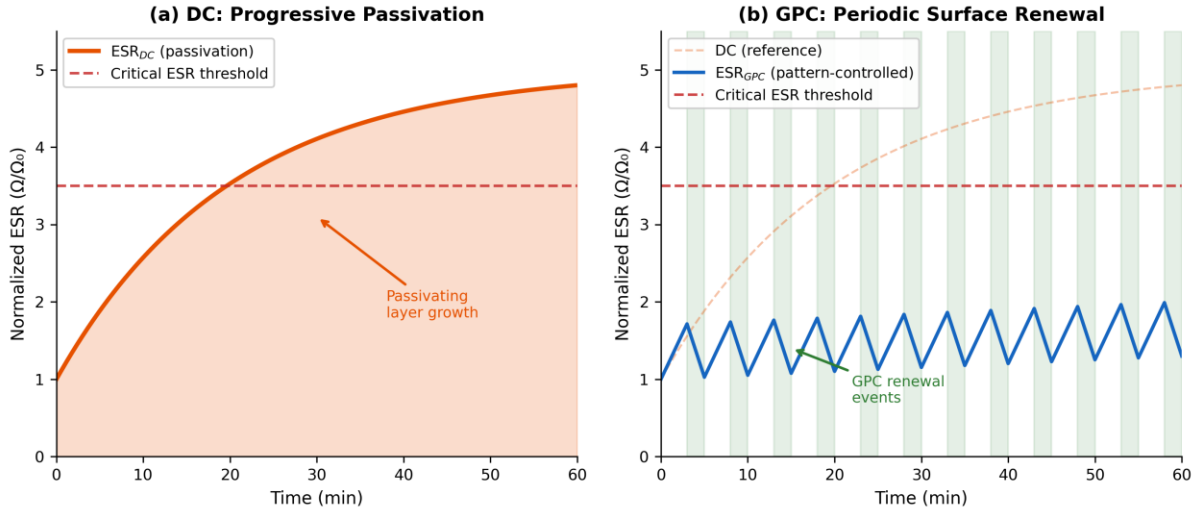

Figure 1. Electrode behavior under direct current versus GPC excitation in electrocoagulation. (a) Progressive passivation layer formation under direct current, showing increasing surface resistance over time. (b) GPC form-driven periodic disruption of the passivating layer, enabling surface renewal and sustained Faradaic efficiency.

Parameter	DC	GPC	Change
Faradaic efficiency (60 min)	~50%	~85%	↑ +35%
Specific energy (kWh/kg removed)	Ref.	~0.65×	↓ ~35%
Cell voltage (at const. ⟨j⟩)	Ref.	↓ 15–25%	↓
Electrode lifetime	Ref.	↑ 1.5–2×	↑
Contaminant removal (equiv. charge)	Ref.	≥ Ref.	≥

Table 1. Comparative performance metrics for direct current versus GPC excitation in electrocoagulation at equivalent average current density. Values represent theoretical predictions derived from the GPC framework; experimental validation is invited using the protocols described in Section 8.

3.3 Heavy Metal and Organic Contaminant Removal

The coagulant generation advantage of GPC translates directly to improved removal of heavy metals, suspended solids, and organic contaminants. Metal cation removal in electrocoagulation follows sweep flocculation kinetics, which are proportional to the coagulant dose [Al^{3+}] or [Fe^{3+}/Fe^{2+}]. At equivalent charge loading (C/L), GPC-driven electrocoagulation achieves a higher effective coagulant concentration due to sustained Faradaic efficiency, yielding superior removal of Pb^{2+}, Cr^{6+}, As, and fluoride in industrial wastewater matrices. For organic contaminants, the elevated bubble production under periodic GPC excitation enhances electroflotation efficiency, accelerating separation of coagulated flocs from the treated water [4].

4. GPC-Enhanced Electrooxidation and Advanced Oxidation Processes

4.1 Hydroxyl Radical Generation Kinetics

Electrooxidation on non-active anodes (BDD, PbO_2, SnO_2) proceeds through the anodic oxidation of water molecules to produce adsorbed hydroxyl radicals at the anode surface:

$$MO\_x + H_2O \rightarrow MO\_x(\bullet OH) + H^+ + e^-$$

The •OH species, once formed, reacts non-selectively with organic pollutants at the electrode surface, mineralizing them to CO_2 and H_2O [9, 10]. The rate of •OH generation is governed by the anodic current density j and the oxygen evolution potential of the electrode material. For a boron-doped diamond anode operating above the oxygen evolution potential (~2.3 V vs. SHE), the •OH generation rate follows a Butler–Volmer-type relationship:

$$r\_\bullet OH = A \cdot \exp(\alpha \cdot F \cdot \eta / R \cdot T)$$

where η is the anodic overpotential, α is the transfer coefficient, F is Faraday's constant, R is the gas constant, and T is temperature. This exponential relationship is strictly convex in η (and hence in j), satisfying the conditions for Jensen's inequality to apply favorably to temporally structured excitation [24].

4.2 GPC Advantage in •OH Generation

Under DC excitation at current density $\bar{j}$, the •OH generation rate is $r(\bar{j})$ evaluated at the steady-state overpotential. Under GPC excitation with a process-specific current form alternating between j_{high} and j_{low} phases at $\langle j \rangle = \bar{j}$, the time-averaged •OH generation rate is:

$$\langle r_{\bullet OH,GPC} \rangle = D \cdot r(j_{high}) + (1-D) \cdot r(j_{low}) > r(\bar{j}) = r_{\bullet OH,DC}$$

where D is the duty cycle of the high-current phase. This inequality, a direct consequence of the convexity of the Butler–Volmer rate expression, quantifies the Jensen gap for •OH production. The magnitude of the improvement scales with the amplitude of the GPC pattern ($j_{high} - j_{low}$) and with the degree of convexity of r(j) at the operating point. Prior experimental validation of pulse-potential electrooxidation has demonstrated energy efficiency improvements of up to 50% relative to DC electrooxidation at the same charge loading [11], consistent with this theoretical prediction.

The second mechanism of GPC advantage in electrooxidation relates to mass transfer. Under DC, the diffusion layer adjacent to the anode thickens over time, limiting the supply of organic substrate to the anode surface where •OH is available for reaction. This mass-transfer limitation reduces the current efficiency (CE) below unity. During the low-current phase of a GPC pattern, the diffusion layer partially relaxes as the concentration gradient at the electrode surface equilibrates toward the bulk. This periodic renewal of the diffusion layer maintains a higher time-averaged substrate concentration at the anode surface, improving CE and reducing the charge required per unit pollutant removal [11, 13].

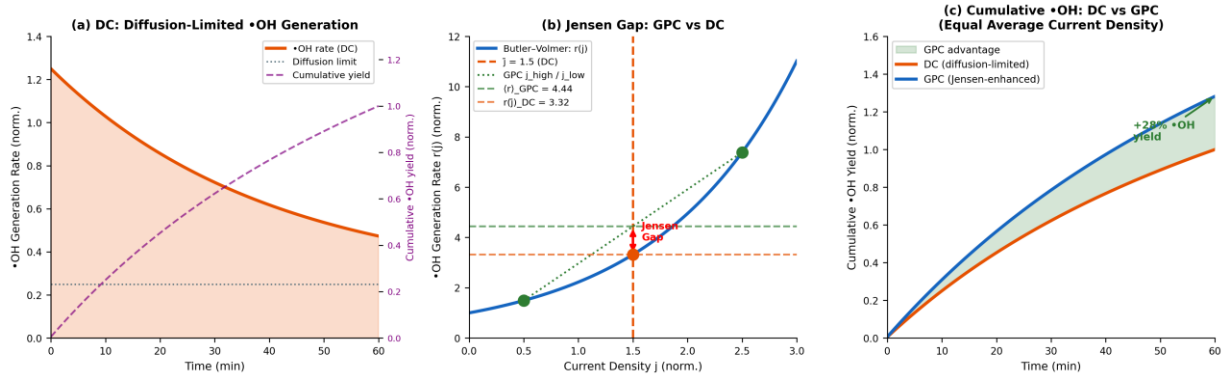

Figure 2. Hydroxyl radical generation under direct current versus GPC excitation in electrooxidation. (a) Direct current generation rate under steady-state diffusion limitation. (b) GPC form cycling between high and low current phases, illustrating the Jensen gap from the convexity of the Butler–Volmer rate expression. (c) Simulated cumulative yield for direct current versus GPC at equal charge loading.

4.3 Electro-Fenton and advanced oxidation process Coupling

GPC is compatible with indirect electrochemical advanced oxidation processes, including electro-Fenton (EF) and persulfate-mediated oxidation. In EF, H_2O_2 is generated at the cathode by two-electron reduction of dissolved O_2, and subsequently reacts with Fe^{2+} to produce •OH via the Fenton reaction. The cathodic H_2O_2 generation rate is nonlinear in cathodic potential, suggesting that GPC patterns applied to the cathodic circuit—structured to optimize two-electron selectivity over four-electron (water) reduction—can enhance H_2O_2 yield per unit energy input. The simultaneous application of GPC patterns to the anodic and cathodic circuits, mediated by the GP R Module system, enables process-specific pattern co-optimization for combined EC–EF or EO–EF configurations [17].

5. GPC-Modulated Electrochlorination

5.1 Chlorine Species Distribution Under DC

Electrochlorination generates disinfectant species—primarily Cl_2, HOCl, and OCl^-—through the anodic oxidation of chloride ions:

$$2Cl^- \rightarrow Cl_2 + 2e^- \ \text{(anode)}; \ Cl_2 + H_2O \rightleftharpoons HOCl + H^+ + Cl^-$$

Under DC operation at elevated current densities or extended treatment times, the initially generated HOCl undergoes further anodic oxidation to chlorate (ClO_3^-) and perchlorate (ClO_4^-)—species that are toxic at regulatory threshold concentrations [15, 16]. This over-oxidation pathway is a function of the integrated anodic charge passed and the local chlorine concentration at the anode surface. The sequential nature of the over-oxidation reactions ($HOCl \rightarrow ClO_3^- \rightarrow ClO_4^-$) implies that the residence time of chlorine species at the anode surface under DC conditions is a critical determinant of product selectivity.

5.2 GPC Selectivity Control

GPC provides a mechanism for temporal control of chlorine species distribution by engineering the anodic residence time at high potential. A GPC pattern configured with short, high-amplitude anodic pulses followed by extended off-phases limits the cumulative anodic charge applied to a

given volume of electrolyte at the electrode surface, suppressing the kinetic pathway to ClO_3^- formation. During the off-phase, the locally enriched HOCl concentration equilibrates with the bulk solution and diffuses away from the electrode surface, reducing the probability of sequential over-oxidation. The GPC pattern parameters—pulse duration τ_on, off-phase duration τ_off, and amplitude ratio j_high/j̄—can be pre-engineered for the chloride concentration and temperature of the feed water to maximize free chlorine yield while maintaining ClO_3^- and ClO_4^- concentrations below WHO guideline values of 700 µg/L and 70 µg/L, respectively [16].

For electrochlorination, the process-specific GPC form encodes explicit knowledge of the chlorine evolution mechanism—rate constants, activation energies, and species diffusivities—into the form geometry, providing a chemistry-informed temporal excitation profile that cannot be achieved by generic pulsing approaches.

6. GPC in Electrodialysis Desalination and Ion Separation

6.1 Concentration Polarization and Membrane Fouling Under DC

Electrodialysis operates by driving ions through selective ion-exchange membranes under the influence of an applied electric field, producing a diluate (desalted) and concentrate stream [17]. Under DC operation, the continuous directional ion flux creates concentration polarization at the membrane/solution interface: the diluate boundary layer becomes depleted of ions while the concentrate boundary layer accumulates them beyond solubility limits. concentration polarization increases the electrical resistance of the stack, reduces current efficiency, and promotes precipitation of inorganic scalants ($CaCO_3$, $CaSO_4$, $Mg(OH)_2$) and organic foulants on the membrane surface, degrading both permselectivity and membrane lifetime [17, 18, 19, 20].

Prior work applying intermittent current interruptions in electrodialysis has demonstrated that periodic off-phases allow the concentration polarization boundary layers to partially relax by diffusion, reducing the interfacial concentration gradient and suppressing scale nucleation [17, 20]. Energy consumption reductions of 30–36% and substantial decreases in membrane scaling have been reported for optimized intermittent-current configurations [20, 24]. These results confirm that the temporal structure of current is a decisive process variable in electrodialysis—the mechanistic basis on which GPC operates.

6.2 GPC Advantage in electrodialysis: Beyond Simple Pulsing

Simple intermittent-current operation in electrodialysis—a rectangular on/off current profile—is a special case of the broader GPC framework. Such approaches do not encode knowledge of the specific ion transport dynamics, membrane properties, or scale-forming species concentrations of the feed water. Suboptimal on/off timing leads to either insufficient concentration polarization relaxation (too-short pauses) or unacceptably long treatment times (too-long pauses), as the energy-time tradeoff noted in the literature implies [18, 22].

GPC in electrodialysis extends simple intermittent-current operation to a multi-parameter engineering space. The process-specific GPC form for electrodialysis encodes the Nernst–Planck ion transport equations and the characteristic times of concentration polarization formation ($\tau_{CP} \propto \delta^2/D_{ion}$, where δ is the boundary layer thickness and D_{ion} is the diffusion coefficient of the limiting ion) and scale nucleation (τ_{scale}) directly into the pattern geometry. The resulting GPC pattern provides:

(i) A high-current excitation phase of duration $\tau_{on} < \tau_{scale}$, ensuring that salt concentrations in the concentrate boundary layer do not exceed solubility before concentration polarization relief;

(ii) A structured low-current or off-phase of duration $\tau_{off} \approx \tau_{CP}$, allowing the boundary layer to relax to a degree sufficient to prevent scale nucleation in the subsequent pulse;

(iii) An optional low-amplitude maintenance current during the off-phase, preventing back-diffusion of already-separated ions while consuming minimal energy—a strategy identified as theoretically advantageous in 1D PEF modeling [18].

The theoretical desalination rate under GPC, integrated over the pattern period T_p, equals that of continuous DC at the same average current density $\langle j \rangle$ by the Faraday charge equivalence. However, the specific energy consumption per unit desalination (SEC, kWh/m³) is lower because: (a) the average cell voltage $\langle V_{cell} \rangle$ at $\langle j \rangle$ is lower under GPC than DC due to reduced stack resistance from concentration polarization mitigation; and (b) membrane lifetime is extended by suppression of scaling, reducing capital cost per unit treated volume [19, 20, 21].

7. GP R Module: Industrial Retrofit Implementation for Water Treatment

7.1 Retrofit Architecture

The GP R Module is a compact industrial edge control unit that implements the GPC framework as a plug-and-play retrofit device for existing electrochemical water treatment infrastructure. The GP R Module interfaces with any standard industrial rectifier through its external reference input, requiring only current and voltage sensing at the rectifier output terminals. No modification of the electrochemical cell, electrode configuration, electrolyte, or process plumbing is required. The GPC pattern appropriate to the target process—EC, electrooxidation, electrochlorination, or electrodialysis—is pre-loaded as a firmware configuration into the module's LUT prior to deployment. Process-specific GPC forms can be updated in deployed units, enabling remote process optimization without on-site hardware intervention. The closed-loop controller tracks the target process state using impedance $Z(\omega)$, ESR, and stress index σ metrics and adjusts pattern scalar parameters (A, I_0, D) in real time.

For electrocoagulation applications, the GP R Module monitors the electrode ESR as a proxy for passivation layer thickness, triggering a pattern transition to the depassivation phase when ESR exceeds a configurable threshold. For electrooxidation applications, the GP R Module tracks the electrochemical stress index $\sigma = dESR/dt$ as an indicator of anode fouling onset. For electrodialysis, the GP R Module monitors stack resistance as a measure of concentration polarization accumulation, adjusting the off-phase duration τ_off dynamically to maintain the stack resistance below the scaling threshold.

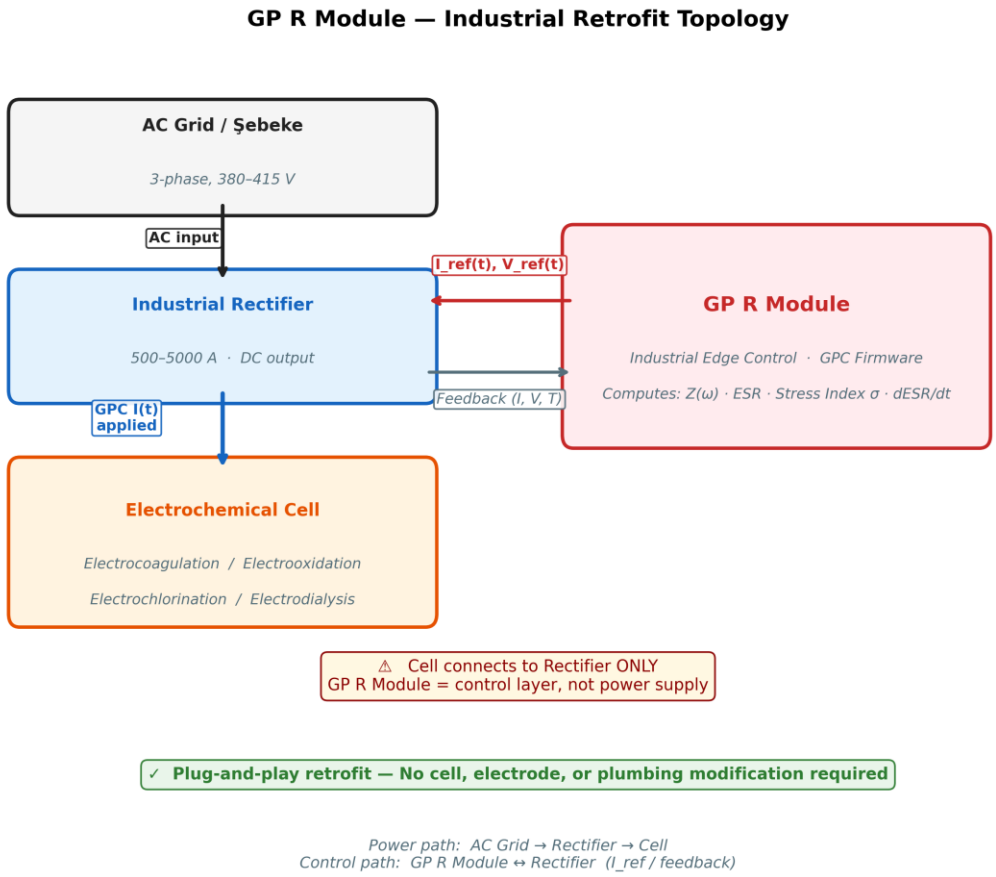

Figure 3. GP R Module industrial retrofit topology for electrochemical water treatment. Power path: AC Grid → Rectifier → Cell. Control path: GP R Module ↔ Rectifier (I_ref / feedback). The cell connects to the rectifier only. No cell, electrode, or plumbing modification is required.

7.2 Process-Specific GPC Form Design for Water Treatment

For each water treatment process domain, the GP R Module executes a process-specific GPC form engineered from first principles. The GPC form for electrocoagulation is designed around the characteristic time constants of oxide layer nucleation and electrolyte replenishment at the sacrificial electrode surface, with excitation and rest phases calibrated to prevent passivating layer accumulation while preserving net anodic dissolution. The GPC form for electrooxidation is derived from the convexity of the Butler–Volmer rate expression at the target anodic overpotential, with phase amplitudes engineered to maximize the Jensen gap in hydroxyl radical generation. The GPC form for electrochlorination is constructed from the sequential kinetics of chlorine species

oxidation, with excitation duration constrained to suppress the over-oxidation pathway to chlorate. The GPC form for electrodialysis is derived from the Nernst–Planck ion transport equations and the characteristic time of concentration polarization layer formation, with off-phase duration calibrated to allow boundary layer relaxation without permitting scale nucleation. All GPC forms preserve the time-averaged current ⟨I(t)⟩ = I_target. Each process-specific GPC form is loaded into the GP R Module as a firmware configuration and is updatable as process parameters evolve.

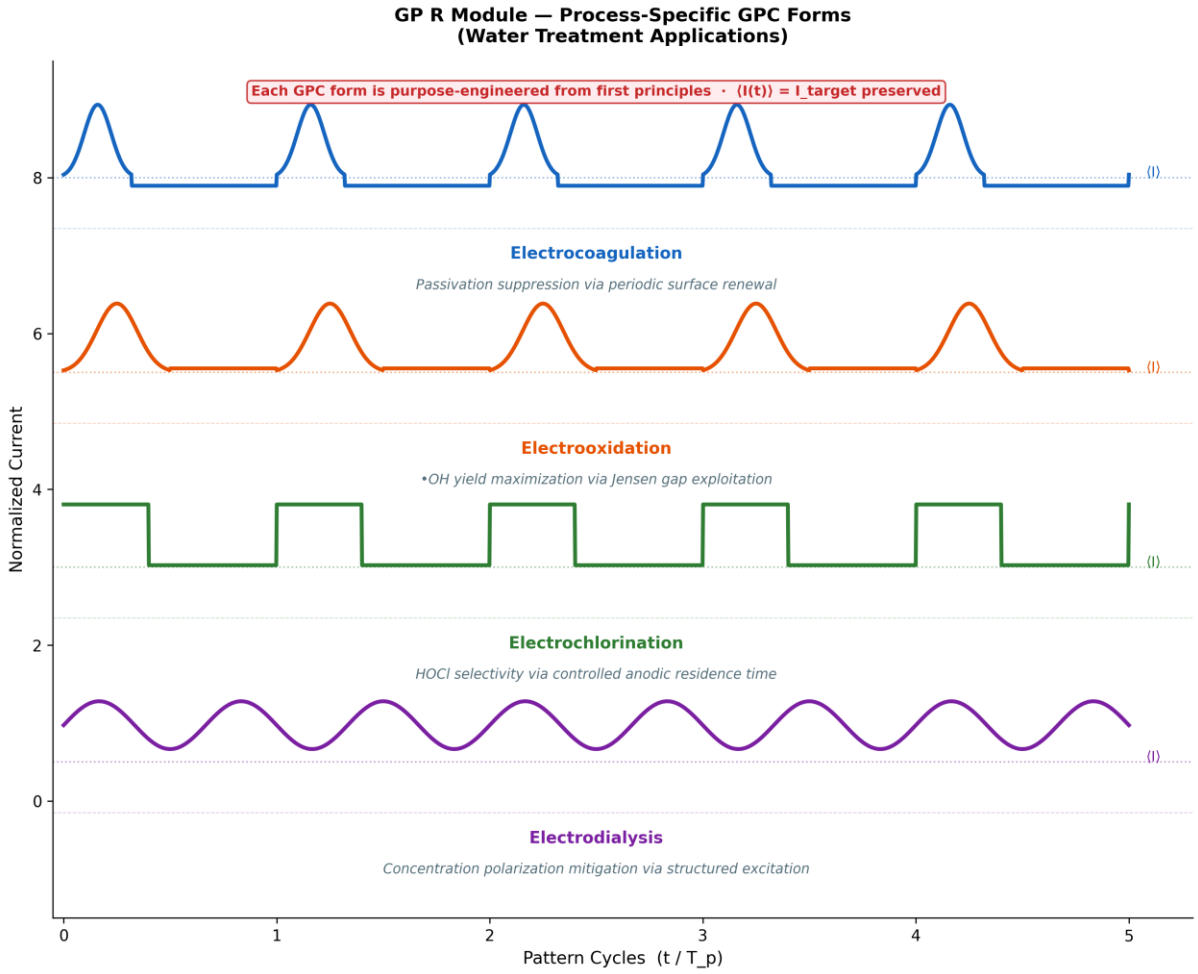

Figure 4. Process-specific GPC forms for the four electrochemical water treatment domains. Each form is purpose-engineered from first principles based on the reaction kinetics, mass-transfer time constants, and interfacial dynamics of the target process. Time-averaged current is preserved across all forms.

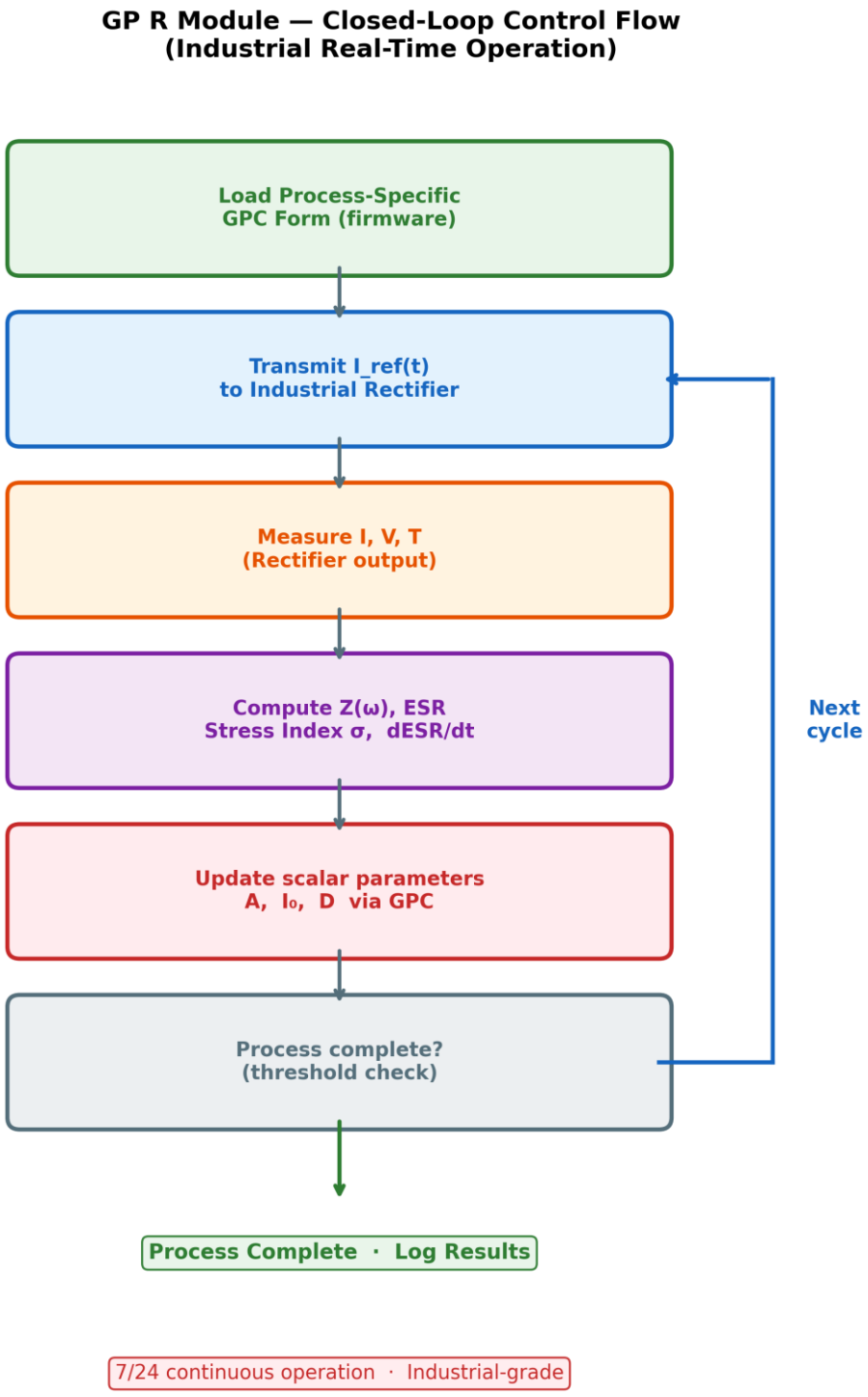

Figure 5. GP R Module closed-loop control flow for industrial real-time operation. The module loads the process-specific GPC form, transmits I_ref(t) to the rectifier, measures process feedback, computes impedance Z(ω), ESR, stress index σ, and dESR/dt, and updates scalar parameters A, I_0, and D via the GPC algorithm. The cycle repeats until process completion criteria are met.

8. Experimental Validation Framework

The GPC framework for electrochemical water treatment constitutes an open experimental platform. The theoretical predictions presented in this paper are directly testable by any research group with access to standard electrochemical equipment. The GP R Module provides a reference implementation for industrial-scale validation by interfacing with existing rectifier infrastructure; laboratory-scale validation requires only a programmable power supply capable of tracking an external current reference signal. The experimental protocols are instrument-agnostic.

8.1 Electrocoagulation Validation Protocol

Proposed experimental protocol: (1) Establish direct current electrocoagulation baseline at current density $\bar{j}$ with aluminum or iron electrodes in a representative wastewater matrix (synthetic or real). Record cell voltage, coagulant generation rate (by ICP-MS), contaminant removal efficiency (COD, turbidity, heavy metal concentration), electrode mass loss, and specific energy consumption (kWh/kg removed) over a 60-minute operation period. (2) Repeat with GPC electrocoagulation using the process-specific GPC form at identical $\langle j \rangle$. (3) Key measurements: ESR evolution (proxy for passivation), Faradaic efficiency (by ICP-MS vs. theoretical dissolution), V_cell time series, and sludge morphology (SEM). GPC prediction: reduced ESR accumulation rate, higher Faradaic efficiency, lower V_cell at equivalent $\langle j \rangle$, and equivalent or superior contaminant removal.

8.2 Electrooxidation Validation Protocol

Proposed experimental protocol: (1) direct current electrooxidation baseline on a boron-doped diamond or dimensionally stable anode anode in a model pollutant solution (benzoic acid or pharmaceutical compound at 20–50 mg/L). Record •OH production rate (via spin-trap EPR or fluorescent probe), current efficiency, chemical oxygen demand removal rate, and energy efficiency (EE/O, kWh/order/m³). (2) GPC electrooxidation with the process-specific GPC form at identical $\langle j \rangle$. (3) Key metrics: EE/O improvement (GPC prediction: 20–50% based on [11]), current efficiency at different organic loading levels, and Tafel slope analysis before and after treatment.

8.3 Electrochlorination Validation Protocol

Proposed experimental protocol: (1) DC electrochlorination in NaCl solution (0.1–1.0 M) on Ti/RuO_2 anode. Measure free chlorine (DPD method), ClO_3^- (IC), and ClO_4^- (IC) as a function of charge passed. (2) GPC electrochlorination with the process-specific GPC form at identical ⟨j⟩. (3) Key metric: free chlorine/ClO_3^- selectivity ratio (GPC prediction: improved free chlorine selectivity with reduced ClO_3^- at equal charge loading).

8.4 Electrodialysis Validation Protocol

Proposed experimental protocol: (1) DC-ED of synthetic brackish water (5 g/L NaCl + scaling-tendency additives $CaCl_2$ + $MgSO_4$) in a laboratory-scale stack. Record stack resistance, desalination rate (conductivity), SEC (kWh/m^3), and membrane scaling (by SEM/EDX after 8-hour operation). (2) GPC electrodialysis with the process-specific GPC form at identical ⟨j⟩. (3) Key metrics: SEC reduction (GPC prediction: 20–35%), membrane scaling index, and demineralization rate per energy unit.

9. Discussion

The theoretical framework presented in this paper unifies four distinct electrochemical water treatment domains under a single mechanistic principle: the exploitation of nonlinear electrochemical response through pre-engineered temporal current structure. The GPC/DDPC framework extends prior work on pulsed DC and polarity reversal in electrocoagulation, pulse-potential electrooxidation, and pulsed electrodialysis by providing a systematic, chemistry-informed approach to pattern design that supersedes empirical trial-and-error optimization of pulse/pause timing.

The Jensen gap analysis provides a quantitative basis for predicting the process advantage of GPC over DC at a given operating point. For convex rate-overpotential relationships (EO, electrochlorination kinetics), the gap is positive and scales with the variance of the GPC pattern distribution. For processes where the primary limitation is surface accumulation rather than kinetics (EC passivation, electrodialysis scaling), the GPC advantage arises from the periodic renewal of the electrode or membrane interface, which can be engineered through pattern timing irrespective of the local convexity of the reaction rate.

A critical distinction between GPC and simple pulsing or polarity reversal is the pre-engineering of pattern geometry. Existing pulsed electrocoagulation studies have explored rectangular current pulses with empirically selected on/off ratios [5, 6, 7]; pulse-potential electrooxidation has used sinusoidal or square-wave excitation with frequency optimization [11]. In contrast, GPC patterns are designed from first principles—incorporating electrode kinetics, diffusion layer time constants, passivation thresholds, and scale nucleation rates—into a fixed geometry that is then deployed with scalar feedback control. This design approach eliminates the need for process-specific empirical optimization and provides a transferable template for new application domains.

The GigaPulse Lab platform makes this approach experimentally accessible. Any laboratory with a programmable potentiostat or current source and standard electroanalytical instrumentation can implement and validate GPC patterns for water treatment. The open-framework nature of GPC is a deliberate design choice: the technology is positioned as a research platform that enables independent experimental validation across diverse application contexts, building the scientific literature base necessary for industrial adoption.

10. Conclusion

This paper has presented a unified theoretical framework for the application of Generated Pattern Current (GPC) across four principal electrochemical water treatment processes: electrocoagulation, electrooxidation, electrochlorination, and electrodialysis. The framework is grounded in Jensen's inequality for nonlinear systems, which establishes the mathematical basis for the superior process outcomes achievable through temporal current structuring relative to direct current excitation at the same average current density.

For electrocoagulation, GPC suppresses electrode passivation through pre-engineered periodic surface renewal, maintaining Faradaic efficiency and reducing specific energy consumption. For electrooxidation, GPC exploits the convexity of the Butler–Volmer rate expression to elevate time-averaged •OH generation, improving oxidative efficiency for organic pollutant degradation. For electrochlorination, GPC controls the anodic residence time of chlorine species, suppressing the sequential over-oxidation pathway to toxic chlorate and perchlorate. For electrodialysis, GPC

mitigates concentration polarization and membrane scaling through chemistry-informed pulsed excitation that goes beyond simple on/off cycling.

The GP R Module provides a plug-and-play industrial retrofit pathway deployable on existing rectifier infrastructure without hardware modification, alongside a modular laboratory validation platform. Detailed validation protocols for each process domain are proposed, enabling independent experimental confirmation by the research community. The GPC framework is protected under PCT/TR2025/051176 and USPTO 19/298,223, with priority date July 23, 2025. The inventor welcomes collaboration with research groups seeking to validate GPC across the water treatment domain.

Acknowledgments

The author acknowledges the foundational contributions of the electrochemical engineering community to the understanding of electrode passivation, reactive species generation, and ion transport in the processes described herein. No external funding was received for this theoretical work.

Declaration of Competing Interest

Ibrahim Karakoc holds the intellectual property and commercial rights through GigaPulse Energy, Izmir, Turkey.

Data Availability Statement

No experimental data were generated or analyzed in this study. This paper presents a theoretical framework. Data sharing is not applicable.

Declaration of Artificial Intelligence and Automated Tools

During the preparation of this work, the author used AI-assisted writing tools for language editing and structural review. The author reviewed and edited all content and takes full responsibility for the integrity and accuracy of the published work.

References

[1] M. Ingelsson, N. Yasri, E.P.L. Roberts, 'Electrode passivation, faradaic efficiency, and performance enhancement strategies in electrocoagulation—a review,' Water Res., vol. 187, p. 116433, 2020.

[2] S. Garcia-Segura, M. Eiband, J.V. de Melo, C.A. Martínez-Huitle, 'Electrocoagulation and advanced electrocoagulation processes: A general review,' J. Electroanal. Chem., vol. 801, pp. 267–299, 2017.

[3] P.V. Nidheesh, M. Zhou, M.A. Oturan, 'An overview on the removal of synthetic dyes from water by electrochemical advanced oxidation processes,' Chemosphere, vol. 197, pp. 210–227, 2018.

[4] A. Shahedi et al., 'A review on industrial wastewater treatment via electrocoagulation processes,' Curr. Opin. Electrochem., vol. 22, pp. 154–169, 2020.

[5] H. Chow, A.L. Pham, 'Mitigating electrode fouling in electrocoagulation by means of polarity reversal,' Water Res., vol. 196, p. 117015, 2021.

[6] Y.E. Durna, A. Bektas, S. Karagöz, 'The role of the current waveform in mitigating passivation and enhancing electrocoagulation performance: A critical review,' Chemosphere, vol. 311, p. 137094, 2023.

[7] P.T.P. Aryanti et al., 'Energy efficiency in electrocoagulation processes for sustainable water and wastewater treatment,' J. Environ. Chem. Eng., vol. 12, p. 113919, 2024.

[8] C.A. Martínez-Huitle, M. Panizza, 'Electrochemical oxidation of organic pollutants for wastewater treatment,' Curr. Opin. Electrochem., vol. 11, pp. 62–71, 2018.

[9] I. Sirés, E. Brillas, M.A. Oturan, M.A. Rodrigo, M. Panizza, 'Electrochemical advanced oxidation processes: today and tomorrow,' Environ. Sci. Pollut. Res., vol. 21, pp. 8336–8367, 2014.

[10] B.P. Chaplin, 'Critical review of electrochemical advanced oxidation processes for water treatment applications,' Environ. Sci. Process. Impacts, vol. 16, pp. 1182–1203, 2014.

[11] Z. He et al., 'Increased energy efficiency using pulse-potential electrochemical advanced oxidation processes,' Chemosphere, vol. 362, p. 142718, 2024.

[12] M.D. Hand, R.D. Cusick, 'Electrochemical disinfection in water and wastewater treatment: identifying impacts of water quality and operating conditions on performance,' Environ. Sci. Technol., vol. 55, pp. 3470–3482, 2021.

[13] M.D. Alam, A. Das, A. Adak, 'Hydroxyl and sulfate radicals-based electrochemical advanced oxidation process for treating dye-bearing wastewater,' Water Pract. Technol., vol. 19, pp. 4816–4838, 2024.

[14] S.A. Kamal et al., 'Enhancing seawater desalination efficiency through optimized pulsed electric field parameters in electrodialysis,' J. Eng. Appl. Sci., 2024.

[15] M.T. Bao, K.T. Wen, D.M. Thompson, 'Design and operating parameters affecting an electrochlorination system,' J. Ind. Eng. Chem., vol. 18, pp. 164–170, 2012.

[16] S.K. Otter et al., 'Approaching easy water disinfection for all: Can in situ electrochlorination outperform conventional chlorination under realistic conditions?' Water Res., vol. 248, p. 120849, 2024.

[17] S. Honarparvar et al., 'Investigation of pulsed electric field operation as a chemical-free anti-scaling approach for electrodialysis desalination of brackish water,' Desalination, vol. 548, p. 116278, 2023.

[18] A. Nikonenko et al., 'Theoretical study of the influence of electroconvection on the efficiency of pulsed electric field modes in electrodialysis desalination,' Membranes, vol. 14, p. 247, 2024.

[19] N. Cifuentes-Araya, G. Pourcelly, L. Bazinet, 'Impact of pulsed electric field on electrodialysis process performance and membrane fouling,' J. Colloid Interface Sci., vol. 361, pp. 79–89, 2011.

[20] A. Campione et al., 'A comprehensive investigation of performance of pulsed electrodialysis for desalination of brackish water,' Desalination, vol. 548, p. 116244, 2022.

[21] V. Nikonenko et al., 'Mitigation of membrane scaling in electrodialysis by electroconvection enhancement, pH adjustment and pulsed electric field application,' J. Membr. Sci., vol. 549, pp. 167–182, 2018.

[22] A.J. Bard, L.R. Faulkner, Electrochemical Methods: Fundamentals and Applications, 2nd ed., Wiley, 2001.

[23] J. Newman, K.E. Thomas-Alyea, Electrochemical Systems, 3rd ed., Wiley, 2004.

[24] N. Wolff et al., 'Understanding nonlinearity in electrochemical systems,' Eur. Phys. J. Spec. Top., vol. 227, pp. 2617–2640, 2019.

[25] I. Karakoc, 'Generated Pattern Current: A Unified Electrochemical Control Framework,' SSRN 6387818, 2026.

[26] I. Karakoc, 'GPC-Based Battery Formation Protocol,' SSRN 6392399, 2026.

[27] I. Karakoc, 'GPC-Based Battery Optimization,' SSRN 6392719, 2026.

[28] I. Karakoc, 'GPC for Electroplating,' SSRN 6439004, 2026.

[29] I. Karakoc, 'GPC for Water Electrolysis,' SSRN 6441898, 2026.

[30] I. Karakoc, 'GPC for Electrochemical Synthesis,' SSRN 6465419, 2026.